AD-A096 375 PENNSYLVANIA STATE UNIV UNIVERSITY PARK MATERIALS RE--ETC F/G 20/2
SINGLE CRYSTAL SUBSTRATES FOR SURFACE ACOUSTIC WAVE DEVICES.(U)
JAN 81 G R BARSCH, K E SPEAR F19628-79-C-0036

UNCLASSIFIED RADC-TR-80-398 NL

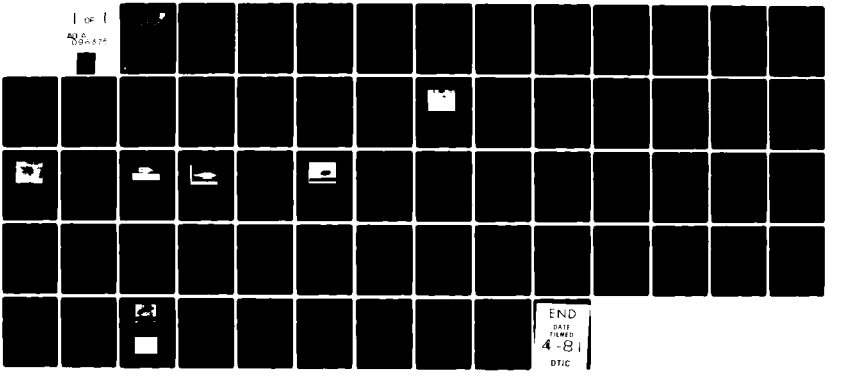

RADC-TR-80-398
Final Technical Report
January 1981

SINGLE CRYSTAL SUBSTRATES FOR SURFACE ACOUSTIC WAVE DEVICES

Pennsylvania State University

G. R. Barsch
K. E. Spear

ROME AIR DEVELOPMENT CENTER
Air Force Systems Command
Griffiss Air Force Base, New York 13441

This report has been reviewed by the RADC Public Affairs Office (PA) and is releasable to the National Technical Information Service (NTIS). At NTIS it will be releasable to the general public, including foreign nations.

RADC-TR-80-398 has been reviewed and is approved for publication.

APPROVED: Paul H. Carr

PAUL H. CARR
Project Engineer

APPROVED: Philipp Blacksmith

PHILIPP BLACKSMITH, Acting Chief
Electromagnetic Sciences Division

FOR THE COMMANDER: John P. Huss

JOHN P. HUSS
Acting Chief, Plans Office

If your address has changed or if you wish to be removed from the RADC mailing list, or if the addressee is no longer employed by your organization, please notify RADC (EEAC) Hanscom AFB MA 01731. This will assist us in maintaining a current mailing list.

Do not return this copy. Retain or destroy.

UNCLASSIFIED

SECURITY CLASSIFICATION OF THIS PAGE (When Data Entered)

REPORT DOCUMENTATION PAGE

READ INSTRUCTIONS BEFORE COMPLETING FORM

1. REPORT NUMBER: RADC-TR-80-398	2. GOVT ACCESSION NO.: AD-A096 375
3. RECIPIENT'S CATALOG NUMBER	
4. TITLE (and Subtitle): SINGLE CRYSTAL SUBSTRATES FOR SURFACE ACOUSTIC WAVE DEVICES.	5. TYPE OF REPORT & PERIOD COVERED: Final Technical Report. 1 Jan 79 — 30 Jun 80
	6. PERFORMING ORG. REPORT NUMBER: N/A
7. AUTHOR(s): G. R. Barsch, K E. Spear	8. CONTRACT OR GRANT NUMBER(s): F19628-79-C-0036
9. PERFORMING ORGANIZATION NAME AND ADDRESS: The Pennsylvania State University, Materials Research Laboratory, University Park PA 16802	10. PROGRAM ELEMENT, PROJECT, TASK AREA & WORK UNIT NUMBERS: 62702F, 23050525, J5
11. CONTROLLING OFFICE NAME AND ADDRESS: Deputy for Electronic Technology (RADC/EEAC), Hanscom AFB MA 01731	12. REPORT DATE: January 1981
	13. NUMBER OF PAGES: 63
14. MONITORING AGENCY NAME & ADDRESS (if different from Controlling Office): Same	15. SECURITY CLASS. (of this report): UNCLASSIFIED
	15a. DECLASSIFICATION/DOWNGRADING SCHEDULE: N/A

16. DISTRIBUTION STATEMENT (of this Report)

Approved for public release; distribution unlimited.

17. DISTRIBUTION STATEMENT (of the abstract entered in Block 20, if different from Report)

Same

18. SUPPLEMENTARY NOTES

RADC Project Engineer: Dr. P. H. Carr (RADC/EEAC)

19. KEY WORDS (Continue on reverse side if necessary and identify by block number)

Crystal Growth; Ultrasonics; Elastic Constants; Thermoelastic Constants; Piezoelectric Constants; Temperature Compensated Materials; Surface Acoustic Wave Devices; Berlinite; Lead Potassium Niobate; Lead Bismuth Niobate, Lithium Metasilicate, Bismuth Molybdate, Bismuth Titanate

20. ABSTRACT (Continue on reverse side if necessary and identify by block number)

In order to search for new temperature compensated materials for surface acoustic wave (SAW) devices with low ultrasonic attenuation and high electromechanical coupling, the following experimental and theoretical investigations were carried out:

(Cont'd)

DD FORM 1 JAN 73 1473 EDITION OF 1 NOV 65 IS OBSOLETE

UNCLASSIFIED

SECURITY CLASSIFICATION OF THIS PAGE (When Data Entered)

(i) Crystal growth research centered around: (a) designing, constructing, and writing the software for a computer controlled constant-diameter attachment for our Czochralski crystal pullers; (b) a major experimental effort on the growth of lead potassium niobate (PKN); $Pb_2KNb_5O_{15}$, and lead bismuth niobate (PBN) $PbBi_2Nb_2O_9$; and (c) a minor experimental effort on the growth of lithium metasilicate, Li_2SiO_3; and bismuth molybdate, Bi_2MoO_6. The use of the constant-diameter control equipment in the crystal growth of these materials resulted in marked improvements, but did not eliminate, the persistent cracking problem. For PKN, a few large crystals suitable for measurements were obtained, and a systematic approach to solving the complex growth problems is proposed. The PBN crystal growth was less of a problem, and more than a dozen single crystal samples suitable for property measurements were obtained. Single domain lithium metagermanate seed crystals were used in attempts to grow single domain lighium metasilicate crystals.

(ii) The dielectric constants ϵ_{11}^T and ϵ_{33}^T and the associated loss tangents of ϕ-berlinite were measured at eleven frequencies from 10^2 to 10^5 Hz between -150 and 200°C. The temperature dependence of, ϵ_{11}^T and ϵ_{33}^T and the relaxation behavior are similar to the results obtained earlier, but the absolute values are 20 to 30 percent smaller than reported previously.

The electrical resistivity of α-$AlPO_4$ was measured as a function of temperature. On the basis of these results it is concluded that the bulk electrical conductivity cannot account for any of the dielectric relaxation phenomena observed earlier which should therefore be attributed to crystal imperfections and/or inclusions.

A dilatometric measurement of the piezoelectric stress constant d_{11} of α-$AlPO_4$ by Uchino and Cross (1979) gives a value about 20 percent smaller than the value previously obtained from ultrasonic measurements and almost three times smaller than the x-ray value. This confirms our earlier prediction that the maximum electromechanical coupling factor of α-$AlPO_4$ should be considerably larger than that of α-SiO_2, but the actual numerical value should be roughly 20 percent smaller than previously predicted.

(iii) The temperature dependence of the two shear modes propagating in [001] has been measured from 10 to 315K for $Bi_4Ti_3O_{12}$. A monotonical decrease of the associated shear moduli has been found. It is only after the remaining seven elastic moduli will have been measured as a function of temperature that the existence of temperature compensated directions for this material can be ascertained.

(iv) Considerable effort was devoted to specimen preparation of lead bismuth niobate which was hampered by the easy cleavage of this material perpendicular to [001]. Property measurements were started. No hysteresis was found at R.T. in the c-direction for an electric field up to 25 kV/cm, indicating either a high coercive field or the absence of a spontaneous polarization in this direction. In the a-direction hysteresis was observed which increased with increasing temperature. The dielectric constant in the a-direction increases by a factor of two from R.T. to 200°C, supporting earlier results which suggest a ferroelectric Curie point at 560°C.

The piezoelectric constant d_{33} of unpoled PBN was determined to be $<10^{-12}$ C/N. The velocities of the three pure acoustic modes propagating in the c-direction have been measured for unpoled PBN as a function of temperature. The results show that the three electric constants c_{33}, c_{55} and c_{66} have the usual negative temperature coefficients.

ACKNOWLEDGEMENTS

The authors would like to thank their colleagues and collaborators for their participation in this work: Dr. M. Brun and Mr. R. S. Berger for the crystal growth investigations, including the construction of the constant diameter control crystal growth equipment, and Dr. Z. P. Chang for the property measurements on berlinite, bismuth titanate and lead bismuth niobate.

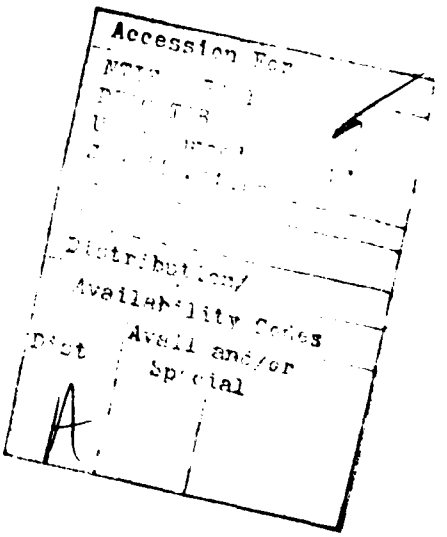

SINGLE CRYSTAL SUBSTRATES FOR SURFACE ACOUSTIC WAVE DEVICES

(TEMPERATURE COMPENSATED PIEZOELECTRIC OXIDE MATERIALS)

Table of Contents

EVALUATION

This is the Final Technical Report on contract F19628-79-C-0036. The objective was to find new temperature compensated materials with [illegible] coupling comparable to lithium niobate. Lead potassium niobate had previously been found to be temperature compensated with 17 times the [illegible] coupling constant of quartz, but large crystal growth was [illegible] by cracking. The use of constant diameter control equipment in the [illegible] lead potassium niobate resulted in marked improvements, but did [illegible] the persistent cracking problem. This problem was discovered to be less severe in lead bismuth niobate. Measurements were initiated towards determining whether this easier-to-grow material is temperature compensated. This research was directed towards eliminating the power consuming ovens presently required in signal processing systems.

Paul H. Carr

PAUL H. CARR
Project Engineer

1. Technical Summary and Progress Report

1.1 Technical Problem and Task Objectives

The objective of the work pursued under this contract is to find new temperature compensated piezoelectric materials for use in ultrasonic SAW signal processing devices, with electromechanical coupling factors comparable to those of $LiNbO_3$, with low ultrasonic attenuation and zero temperature coefficient of the delay time.

1.2 Methodological Approach

The research performed consists of:

(i) Identification of suitable new piezoelectric materials on the basis of heuristic theoretical relations between properties, composition and crystal structure.

(ii) Both exploratory and systematic crystal growth studies on a variety of materials which are expected to possess temperature compensated crystallographic directions and which had been selected earlier on the basis of heuristic criteria (Barsch and Newnham, 1975; Barsch and Spear, 1977).

(iii) Measurement of the single crystal elastic, thermoelastic, piezoelectric and dielectric properties of several promising candidate materials for which suitable single crystals were obtained.

Based on the results obtained under (iii) the existence of temperature compensated cuts for ultrasonic surface waves for the materials studied and their suitability for SAW devices will be investigated by the scientific staff of the Rome Air Development Center under supervision of the Contract Monitor, Dr. P. H. Carr.

1.3 Technical Results

1.3.1 Identification of New Materials

It can be shown by means of a thermodynamic analysis that the piezoelectric constants of ferroelectrics derived from centric prototypes are proportional to the electrostriction constants and the spontaneous polarization. Thus for systematic attempts to find new materials with larger electromechanical coupling factors the microscopic parameters which determine these properties must be well understood. Previous theoretical treatments of electrostriction are inadequate even for such simple solids as alkali halides. Therefore, under a different contract* theoretical work is being pursued in order to develop a more adequate theory of electrostriction, to apply it to alkali halides and to selected classes of piezoelectric and ferroelectric materials. It is hoped that the results will

---

*Targeted Basic Studies of Ferroelectric and Ferroelastic Materials for Piezoelectric Transducer Applications, ONR Contract No. N00014-78-C-0291.

provide heuristic guidelines for maximizing the electrostriction constants and the piezoelectric constants for a given crystal structure. In conjunction with earlier criteria for identifying temperature compensated materials (Barsch and Newnham, 1975) this will hopefully lead to an updated version of our earlier list of potentially temperature compensated materials (Barsch and Newnham, 1975).

1.3.2 Crystal Growth

Crystal growth research centered around: (a) designing, constructing, and writing the software for a computer controlled constant-diameter attachment for our Czochralski crystal pullers, (b) a major experimental effort on the growth of lead potassium niobate (PKN), $Pb_2KNb_5O_{15}$, and lead bismuth niobate (PBN), $PbBi_2Nb_2O_9$, and (c) a minor experimental effort on the growth of lithium metasilicate, Li_2SiO_3, and bismuth molybdate, Bi_2MoO_6.

1.3.2.1 Constant-Diameter Control Equipment

In an attempt to reduce and hopefully eliminate the persistant cracking in PKN and other oxide crystal boules, an automated constant-diameter control system making use of a DEC LSI-11 microcomputer was designed and built for our Czochralski crystal pullers. The system is based on the continuous weighing of the crucible at a constant pulling rate. The difference between the rate of mass loss and a desired rate input into the computer is translated into a temperature correction for the furnace. The temperature of the furnace is the primary experimental parameter which controls the diameter of the crystal boule. The system works essentially as a proportional controller.

The computer programs written for the system allow the experiments to be run in any of three modes: (1) a manual control mode, in which the equipment computes and displays the rate of mass loss from the crucible periodically, and outputs a desired power level signal to the furnace power supply, (2) a constant-diameter mode, in which the equipment calculates the rate of mass loss, compares it to a desired constant rate, and then translates this difference into a power correction to the furnace, and (3) a programmed shape mode, in which the equipment controls the initial necking down of the boule, its expansion, the constant diameter region, and the final tapering of the crystal before terminating growth. The equipment also controls the cooling of the crystal to room temperature.

1.3.2.2 Lead Potassium Niobate (PKN)

The crystal growth of PKN was continued in an attempt to reduce the persistant cracking problem in the crystal boules. Growth with a precisely controlled platinum-wound resistance furnace and various configurations of heat shielding was pursued, but with limited success. The use of ultra-pure starting materials resulted in more severe cracking, although the quality of the cracked pieces was significantly improved. The rapid cooling through the Curie temperature of PKN resulted in fewer domains. However, the rapid cooling resulted in thermal stresses which produced significant cracking. Various temperature gradients and cooling rates were tried, but again produced limited success in reducing the cracking problem.

An attempt was made to grow PKN crystals hydrothermally below the Curie temperature, but the initial results were not promising, so this effort was dropped.

The most significant improvement in the cracking problem resulted when the constant-diameter control equipment was completed and used with PKN. Although the cracking persisted, a few 5x5x5 mm^3 samples were obtained, and the general quality of the crystals increased.

The cracking problem in PKN is obviously not dominated by one type of experimental parameter, but is a complex combination of factors related to temperature, composition, and boule size and shape. Some of the interrelationships have been defined, and a systematic program for trying to optimize the crystal growth parameters has been outlined.

1.3.2.3 Lead Bismuth Niobate (PBN)

The Czochralski growth of PBN was initiated during this contract. The primary problems encountered were: (1) significant vaporization losses, (2) secondary nucleation during the expansion of the neck region, (3) cracking of the crystal boules, and (4) easy cleavage in the crystal planes parallel to the bismuth oxide layers in the structure.

The first problem was solved by inclosing the crucible region in a fused silica tube closed fairly tightly at both ends. This limited the condensation, and thus the rate of vaporization losses to a tolerable level. The second problem of multiple nucleation is directly related to the significantly slower growth in the c-direction of the crystal, the direction perpendicular to the bismuth oxide layers in the structure. After studying and

defining this problem, we concluded that the only solution is to use slow growth rates when expanding the neck region and to carefully control the temperature.

The third and fourth problems are related in that most of the cracking occurs along the cleavage planes. The stresses which cause the cracking are a result of thermal gradients and the multiple nucleation (and accompanying mismatch of the single crystal grains). The use of the constant-diameter control equipment has largely reduced the cracking from thermal stresses.

Although most PBN crystal boules are cracked and/or contain more than one single crystal domain, more than a dozen high-quality single crystal samples with sizes greater than 5x5x5 mm^3 have been obtained from these experiments.

1.3.2.4 Lithium Metasilicate and Bismuth Molybdate

Crystals of lithium metasilicate grown previously contained 180° twins which could not be removed by poling. In an attempt to grow twin-free crystals, single domain lithium metagermanate single crystal seeds were used. The two materials are isostructural, and their lattice dimensions are similar, so the prospects looked good. The most significant problem has been the lower melting temperatures of the germanate and germanate-silicate solid solutions. Starting the growth of the silicate on the germanate at a slow enough rate for topotaxial growth, and yet fast enough to avoid melting the seed is a problem that is still being examined.

Crystal growth studies on bismuth molybdate were begun as a part of a senior thesis project in Ceramic Science and Engineering at no cost to the present contract. However, the impetus for this project was the promising results we obtained on a previous contract (Barsch and Spear, 1977). These studies have just begun, but it is anticipated that the constant-diameter control equipment will greatly reduce the previous cracking problems which were encountered with this material.

1.3.3 Physical Property Measurements and Suitability for Temperature Compensated SAW Devices

1.3.3.1 α-Berlinite

Some differences among crystals grown at different laboratories are found in the loss tangent, but they should (via the temperature coefficients of the dielectric constants ε_{11} and ε_{33}) have only a relatively small influence on the temperature compensated directions and the maximum attainable electromechanical coupling factor.

The value of d_{11} for α-berlinite measured dilatometrically by Uchino and Cross (1979) on the same crystal as used for the ultrasonic measurements gives a value about 20 percent smaller than the value deduced from the ultrasonic data. Thus the maximum electromechanical coupling factor k of α-berlinite for bulk waves should only be roughly two times larger than for α-quartz and not, as previously predicted, 2.5 times (Chang and Barsch, 1976) or 4.5 times (Barsch and Spear, 1979).

In conjunction with the ultrasonically determined value for d_{11}, the dilatometric results of Uchino and Cross for d_{11}

suggest that the x-ray values of d_{11} and d_{14} are subject to a large systematic error.

1.3.3.7 Bismuth Titanate and Lead Bismuth Niobate

The suitability of bismuth titanate as a substrate for temperature compensated SAW devies cannot yet be decided on the basis of the available ultrasonic data pertaining to only two shear modes.

The availability of sufficiently large single crystals of PBN made it possible to start the investigations and measurements of the propertis of this promising material. The assessment of the suitability of this material as a substrate for temperature compensated SAW devices must await the completion of these studies.

1.4 DOD Implications

Present and future engineering applications of SAW devices include military (and civilian) communications and Radar systems, such as multichannel communications, secure anti-jam communication for satellites, miniature avionics and electromagnetic counter measures. The main performance limiting factor of current SAW devices is that it has not been possible to simultaneously achieve broad bandwidth which increases with increasing electromechanical coupling factor, and small temperature coefficient of time delay. For applications where temperature compensated performance is essential, as in SAW code correlators and in circulating store devies, quartz has been used as a substrate material, which has a relatively small bandwidth.

For two of the materials investigated under the present contract one may expect the existence of temperature compensated cuts for bulk and surface waves, with substantially larger electromechanical coupling, and bandwidth than for α-quartz. For one of the materials investigated, berlinite, temperature compensated cuts with electromechanical coupling factors for bulk waves two times larger than for quartz may exist. The second material, lead potassium niobate, could be still better. Thus by replacing quartz as a substrate material in suface acoustic wave (SAW) devices with one of these materials insertion losses can be reduced and the operating frequency and/or bandwidth can be increased. In this manner the efficiency, reliability and capability of military communications and Radar systems utilizing SAW signal processing devices can be significantly improved.

1.5 Implications for Further Research

It has been demonstrated that the search for new temperature compensated materials with properties superior to those of α-quartz through the approach used under the present contract can be successful. One may therefore hope that a continued systematic search for new temperature compensated materials under a future contract could lead to the discovery of even more suitable materials. To this end continued crystal growth efforts are required to obtain suitable (single domain) single crystals for the physical measurements which are necessary to assess the use of a given material for SAW device applications.

1.6 Special Comments

No special comments are offered at this time.

2. Crystal Growth Results

The crystal growth efforts pursued under the present contract included both equipment development and crystal growth experiments on four different chemical systems. The equipment development was the design and building of a computer-controlled constant diameter system for our Czochralski crystal puller. The four different crystal systems which were experimentally examined were lead potassium niobate (PKN), $Pb_2KNb_5O_{15}$; lead bismuth niobate (PBN), $PbBi_2Nb_2O_9$; lithium metasilicate, Li_2SiO_3; and bismuth molybdate, Bi_2MoO_6.

The objective was to explore, develop and apply feasible methods for the growth of high-quality single crystals sufficiently large for the physical property measurements. The approach and the results are described below.

2.1 Constant-Diameter Control Equipment

In an attempt to reduce and hopefully eliminate the persistent cracking problem accompanying the crystal growth of lead potassium niobate and other oxide crystals, an automated constant diameter control system was designed and built for our Czochralski crystal pullers. A brief description of the system and the principles behind its operation are given below.

The constant diameter control system employs the method of continuous crucible weighing at a constant pulling rate. The

rate of loss calculated from the crystal density, pulling rate, and desired diameter. Any difference between these two values is translated into a temperature correction for the furnace, which is essentially the same as a correction in the crystal diameter.

The equipment consists of: (i) a Digital Equipment Corp. LSI-11 microcomputer, (ii) a Heath-video terminal and paper tape reader and punch, (iii) a digital-to-analog converter and operational amplifier, and (iv) an Arbor 3006 top-loading electronic balance. A photograph of the completed system is shown in Figure 1.

The LSI-11 computer reads the balance through a custom designed and built interface board. These digital balance readings are time-averaged by the appropriate computer programs, temperature corrections are calculated (in terms of power settings for the furnace), and then this digital signal is converted to an analog signal which is amplified and passed on to the furnace controller. The system works essentially as a proportional controller. The advantage of the digital design, in comparison with an analog design, is its flexibility. All input parameters can be readily adjusted during an experiment, and special correction terms can be easily incorporated into the computer program.

The computer programs used for this system were designed on this contract and are writtin in BASIC, although FORTRAN could also have been used. The program currently being used allows an experiment to be performed in any of three modes: manual, constant diameter, and programmed shape. In the manual mode, the system performs two functions: (1) outputting the desired power

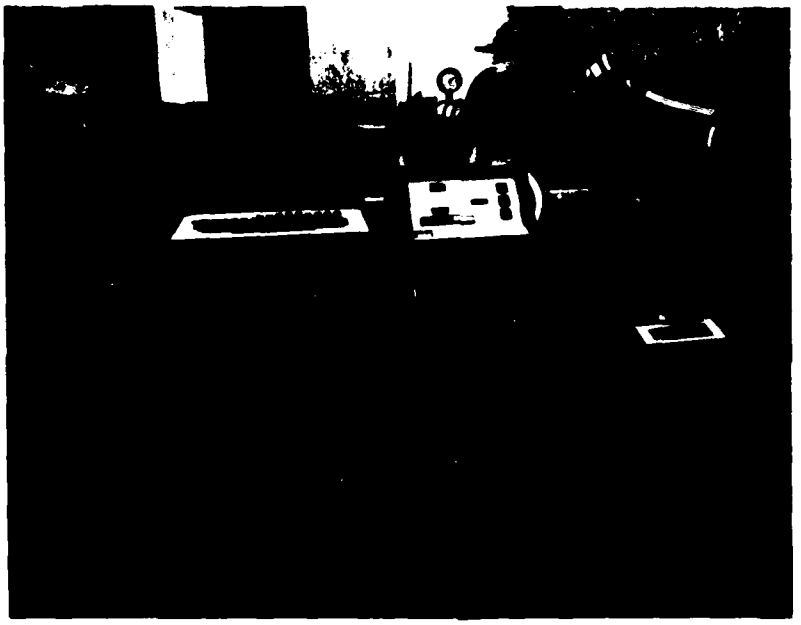

Figure 1. Automatic Diameter Control Crystal Growth Equipment

Instrument rack contains on the top shelf the CRT computer terminal (left) and the paper tape punch/reader (right), on the middle shelf the digital/analog converter and operational amplifier (left) and the LSI-11 micro-computer (right), and on the bottom shelf the digital AD Little induction furnace and the electronic balance (to the right) are visible.

level to the generator, and (2) computing the rate of weight loss in mg/min every two minutes.

In the constant diameter mode, the computer periodically calculates an average rate of weight loss, compares this with the constant desired value, calculates a power correction, and then applies this correction.

In the programmed shape mode, the system performs the same function as in the constant diameter mode in addition to calculating a change in the rate of weight loss as a function of time so that a desired crystal shape can be grown. The growth is automatically controlled from the initial necking down of the polycrystalline boule, to the expansion and constant diameter stage, to the final tapering down of the crystal before the termination of growth. After the crystal is separated from the melt, the computer controlled system also controls the cooling as a function of time.

2.2 Lead Potassium Niobate (PKN)

The crystal growth studies on PKN, $Pb_2KNb_5O_{15}$, begun under previous contracts (Barsch and Spear, 1977, 1979) were continued in an attempt to drastically reduce the cracking problem in the crystal boules.

Since a number of our previously grown PKN crystals contained appreciable amounts of impurities, growth was attempted with high purity starting materials and maximum care to avoid contamination during the preparation of the reacted starting powders. Mixing was performed in plastic ball mills with teflon rollers, and sintering was carried out in covered platinum

crucibles. The ceramic heat shields in the growth furnace were covered with platinum foil to avoid contamination by loose alumina particles. This foil changed the thermal characteristics of the systems so that several experiments had to be performed before decent crystal boules could be grown. The resulting crystals obtained were pale yellow and very transparent, and the quality of the crystals markedly improved. However, the cracking problem persisted, and in fact became worse with the pure starting materials. It was quite obvious that these crystals were very highly strained.

A number of experiments indicated that cooling at relatively rapid rates diminished cracking of the crystals because of the formation of much smaller domains which could withstand the induced stress much better than the intermediate size domains. However, if the crystals are rapidly cooled, there is usually sufficiently large thermal stresses to crack them. To get around this conflict, an attempt was made to cool through the ferroelastic phase transition at an extremely slow rate so that one, or a very few, large domains would be produced and thermal equilibrium would also be approached at all temperatures. A voltage stabilizer was included in the furnace power supply, and the temperature was lowered manually through the transition to avoid temperature fluctuations. The cooling rate was approximately 1/2°/hr. However, the crystal obtained in this experiment was also severely cracked.

An attempt was made to grow PKN crystals hydrothermally at 400°C. This temperature is below the transition temperature, so

cracking caused by the induced stress from the transition would be avoided. A silver-lined autoclave was used for the experiment, with pure water for the solvent. The source material was a sintered pellet of PKN which was placed in the bottom of the vessel. Seed crystals were cut from Czochralski grown boules in the form of thin plates with a- or c-planes as faces. These seeds were suspended by a fine platinum wire in the top of the vessel. The autoclave was then pressurized to 10,000 psi and heated to 400°C for ten days. The temperature at the top of the pressure vessel where the seed crystals were located was 360°C. No measurable growth of the seeds was observed at the end of the experiment, and the crystals and source pellet both had a black layer formed on the surface due to the partial reduction of the lead oxide. Because of these negative results, no further hydrothermal crystal growth experiments on PKN were performed.

Toward the latter part of the present contract period, the constant diameter control equipment was completed and could be used with the growth of PKN. It was hoped that a crystal boule with a constant diameter would contain more uniform thermal gradients during growth and subsequent cooling, and would thus have less tendency for cracking. Several boules were grown with the use of this equipment, both in the constant diameter mode and the controlled shape mode (see previous section). Cracking was reduced, but not eliminated. The general quality of the crystals increased, and a number of crack-free single-crystal regions of approximately 5x5x5 mm^3 were obtained. The lack of time precluded pursuing further research on PKN.

The above results help confirm the conclusion that the

cracking problem in PKN crystals is a complex combination of several factors. The most important factors appear to be (i) the magnitude and uniformity of thermal gradients during growth and cooling cycles, (ii) the number and size of the domains produced at the ferroelastic transition, and (iii) the composition of the crystal. The factors related to thermal gradients and domains are strongly dependent on the physical size and shape (and uniformity of shape) of the crystal, and the thermal gradients and cooling rates of the furnace during an experiment. Although the composition appears to play a role in the cracking problem, the exact nature of this role is not clear. The fact that the more impure crystals were cracked less than those grown with high purity chemicals is probably related to the enhanced nucleation of domains at sites of imperfections. Crystals with a large number of small domains are highly strained, but contain fewer cracks, and the large numbers of domains may be a result of high cooling rates, non-uniform crystal shapes, and/or chemical impurities and physical imperfections.

Sorting out the complex nature of the cracking problem in PKN will require a concentrated effort on the crystal growth of this material. The use of equipment to strictly control the shape of the crystal is an absolute necessity. This problem factor can then be eliminated. Fixing the thermal parameters of the furnace, and then studying the effects of stoichiometry, impurities, and physical defects on the growth should provide the needed insight into the effects of these latter parameters. Next, fixing the chemical and structural parameters at the

optimum values and then studying the effects of thermal parameters in a systematic fashion should help to determine general guidelines for the growth of crack-free crystals. The next step would be to fix both the chemical and structural parameters and the thermal parameters at their optimum conditions, and then to study the effects of crystal size, shape, and uniformity of shape on the cracking. This would complete the first cycle of the study. The cycle should then be repeated in order to approach an optimum set of parameters for the growth of high-quality, crack-free crystals of PKN. The complex interrelationships of the various parameters as they relate to the cracking of PKN crystals makes solving this problem by a less systematic method virtually impossible.

2.3 Lead Bismuth Niobate (PBN)

The crystal growth of $PbBi_2Nb_2O_9$ (PBN) by means of the Czochralski pulling method was initiated during this contract. No previous report of the crystal growth of this compound was found in the literature.

The compound in the form of powdered starting material for the crystal growth was synthesized by prereacting its constituent powdered oxides using standard high temperature sintering techniques. It contained 5 wt % excess of PbO and Bi_2O_3 to compensate for the appreciable volatility of these two components at the crystal growth temperatures. Also because of this volatility problem, a long fused silica tube, fairly tightly closed at both top and bottom, was used to house the crucible in the cold-walled chamber enclosing the rf-heating region.

During the initial growth runs, crystals were nucleated on a platinum wire, and then necked down in an attempt to obtain a single crystal seed. As expected, the fast growth direction was parallel to the bismuth oxide layers in the structure, which are perpendicular to the c-axis. In subsequent experiments, the seeds were oriented so that the fast growth direction and the crystal pulling direction were coincident. Typical pulling rates were 4-6 mm/hr at a rotation rate of 15 rpm.

Crystal boules of PBN are yellow and transparent. In comparison to lead potassium niobate (PKN), the cracking problem in the boules is slight. However, the PBN crystals cleave very easily in the c-planes (the planes parallel to the bismuth oxide layers in the structure). This has been a major problem in preparing crystals for property measurements.

Crystals of PBN are quite sensitive to growth instabilities, as was evidenced by the observed growth defects in crystals grown while the crystal pulling mechanism was not operating properly (the slight "hitch" in the pulling rate was not observable to the eye). Figure 2 shows a thin section of such a crystal which was examined under an optical microscope. The equally spaced defects are about 8μm apart, and are perpendicular to the growth direction.

A major crystal growth problem in the PBN system is inhibiting the nucleation of new crystals when expanding the crystal in the c-direction, the slow growth direction perpendicular to the bismuth oxide layers in the structure. While expanding the crystal diameter from the neck, the slightest

Figure 2

Lamella-type defects in a thin section of lead bismuth niobate as viewed with an optical microscope. Growth rate was 6 mm/hr at 15 rpm. The arrow indicates 200 μm in the growth direction.

temperature instability can cause nucleation of new crystals. Once nucleated, the additional crystals tend to grow the full length of the boule. Figure 3 shows a typical secondary crystal originating at the base of the neck and propagating into the bulk of the crystal. This crystal was grown before the automatic constant diameter equipment was completed.

A large number of PBN crystals were grown with the use of the automatic constant diameter equipment. The first ones were grown using only the constant diameter more, but later crystals were grown completely under the control of this equipment: the initial growth, the necking down and expansion, the constant diameter region, and the tapering of the growth at the end of the run. Multiple nucleation during the neck expansion and cleavage parallel to the growth direction were problems, but more than a dozen single crystal samples greater than 5x5x5 mm^3 are now available for characterization, poling, and property measurements. A typical crystal boule is shown in the photograph given in Figure 4.

2.4 Lithium Metasilicate and Bismuth Molybdate

Extensive crystal growth studies on lithium metasilicate were reported previously by Barsch and Spear (1979). These studies indicated the as-grown crystals of Li_2SiO_3 contained 180° twins. In an attempt to grow untwinned crystals, experiments were performed in which lithium metagermanate (Li_2GeO_3) single domain crystals were used as seeds. The two compounds are isostructural and possess similar lattice dimensions, so it was

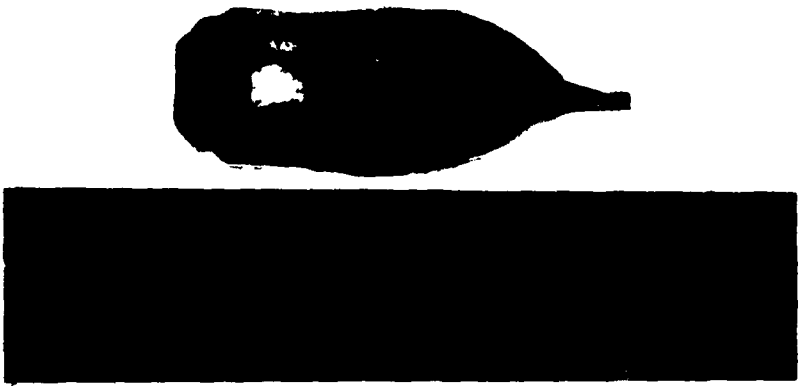

Figure 3. Boule of Lead Bismuth Niobate

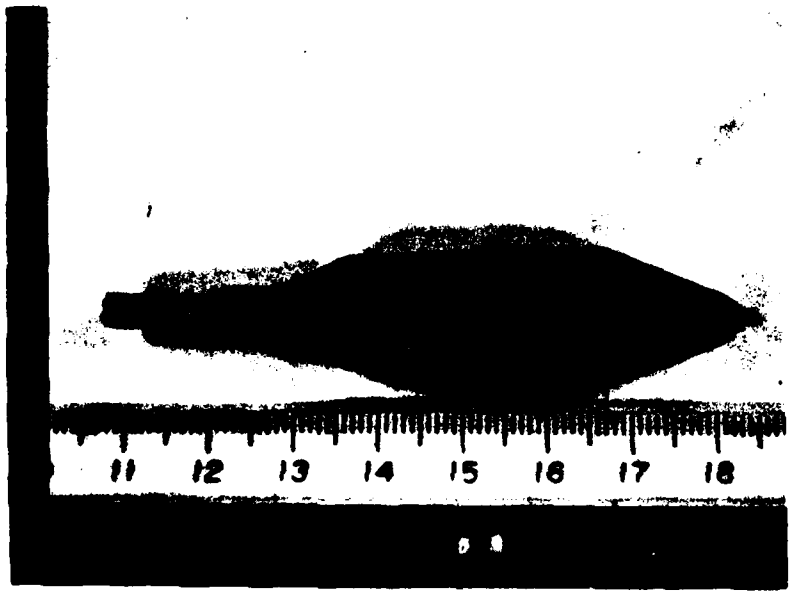

Figure 4

Typical PBN (Lead Bismuth Niobate) Crystal Grown with Constant-Diameter Control Equipment

expected that topotaxial nucleation of the silicate on the germanate would occur quite readily.

A few crystal growth experiments were performed to test the above ideas, but success was limited. A typical boule is shown in Figure 5 along with the germanate seed crystal containing two slits for wiring the seed onto the pulling rod. The initial growth on the seed and the expansion of the boule were performed manually, but the constant diameter region was controlled automatically. The initial growth on the germanate seed is quite tricky since the germanate and germanate-silicate solutions have lower melting temperatures than the silicate. Once the silicate is nucleated and has started to grow, diffusion of the germanate toward the melt-crystal interface is slow enough that this interface is maintained at the melting point of the silicate.

The low density of the lithium metasilicate (2.52 gm/cc) results in mass changes per growth length of the boule which are very close to the sensitivity of our constant diameter control equipment. At the small diameters of the boule near the seed crystal, the equipment cannot be used to automatically expand the diameter.

The germanate seed - silicate boule interface region is still being examined to determine if this approach to growing twin-free lithium metasilicate is worth pursuing.

Crystal growth experiments on bismuth molybdate (Bi_2MoO_6) were begun as a senior thesis project in Ceramic Science and Engineering at Penn State at no personnel cost to the present contract. On a previous Air Force contract (Barsch and Spear, 1977), preliminary crystal growth experiments on bismuth

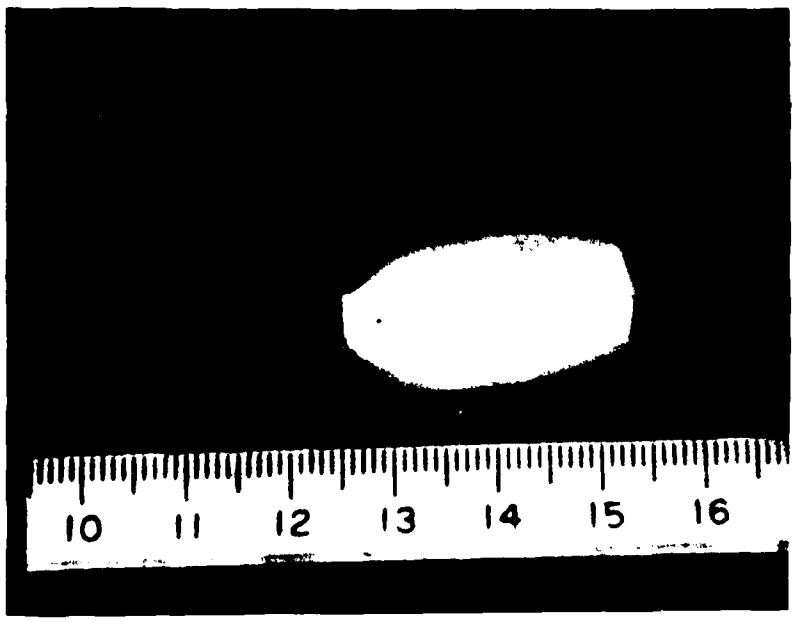

Figure 5

Typical Boule of Lithium Metasilicate Grown on a Single Domain Lithium Metagermanate Seed Crystal

molybd... produced very promising results, although cracking was a prob...m. It is hoped that the new constant diameter control equipment will provide the level of control needed to produce large, high-quality single crystals of this material. At the time this report was written, experiments in which the material was nucleated on a platinum wire had been completed. The boules contained a number of crystals, but sections could be salvaged for use as seeds in subsequent experiments. Without the use of single crystal seed crystals, it is virtually impossible to obtain single crystal boules. Grain boundaries and cracks in the neck region tend to propagate through the entire boule.

3. Elastic, Thermoelastic, Piezoelectric, Dielectric and Electromechanical Properties

3.1 α-Berlinite

3.1.1 Dielectric Properties

Earlier measurements of the dielectric constant ε_{33}^{T} of the associated loss tangent for α-berlinite (Barsch and Spear, 1979) have been repeated and extended to lower frequencies by using a fully automated Hewlett Packard Model 4274A multi-frequency LCR meter. The purpose of these new measurements was to extend the previous measurements to lower frequencies in order to search for a maximum of the high temperature rise of the loss tangent and in order to identify the nature of this loss mechanism. In addition, the aim was to obtain more accurate values for ε_{33}^{T} because the previously reported values were subject to rather large errors because of the small capacitance values of the berlinite platelet used, which were larger, but comparable to the

stray capacitance of the open circuit. The new capacitance bridge used has higher resolution, a larger frequency range at low frequencies, and allows measurement of more intermediate frequencies. Because of the higher resolution the larger stray capacitance can be determined more accurately than with the bridge used previously.

The measurements were mde on an X-cut platelet of thickness 1.025 mm, grown at the U.S. Signal Corps Laboratories, Fort Monmouth, New Jersey, and a Z-cut platelet of thickness 0.0968 mm, grown at the U.S. Naval Weapons Center, China Lake, California. The measurements were made at eleven frequencies (10^2, 1.2×10^2, 2×10^2, 4×10^2, 10^3, 2×10^3, 4×10^3, 10^4, 2×10^4, 4×10^4, 10^5 Hz) as a function of temperature from about -150 to 200°C. All data were taken with decreasing temperature.

In Figures 6 to 10 the results for ε_{11}^T, ε_{33}^T, tan δ_1 and tan δ_3 are shown for five selected frequencies. The data for the lowest frequencies measured have been omitted because of large scatter resulting from poor instrumental resolution. The following major features may be discerned:

(i) Dielectic constant ε_{11}^T. For low frequencies ε_{33}^T increases monotonically with increasing temperature (within the scatter of the experimental data), but with increasing frequency two shallow minima at about -100 to -80°C, and at about 110 to 150°C, and a broad maximum at about 70 to 80°C appear. The temperature at which the low temperature minimum and the maximum occur are almost independent of frequency, but the high temperature minimum is shifted to higher temperature as the frequency increases.

(ii) Dielectric constant ε_{33}^{T}. With the exception of a very shallow low temperature minimum at high frequencies, ε_{33}^{T} increases monotomically with increasing temperature and exhibits the broadened step-like increase characteristic of a single relaxation mechanism.

(iii) Loss Tangent tan δ_1. The los tangent for δ_1 shows a continuous rise with increasing temperature, superimposed on which are two relaxation peaks of approximately constant height. The continuously rising part increases with decreasing frequency, but even at the lowest frequency of 200 Hz no maximum is reached. Since measurements of the electrical conductivity of this sample (Section 1.3.3.1.2) suggest that the dielectric loss contribution arising from the electrical conductivity is much smaller than the measured loss this feature must be attributed to a defect relaxation mechanism, and a maximum is to be expected at still lower frequency with decreasing frequency. The two small relaxation peaks are shifted toward lower temperature, as is to be expected for a relaxation mechanism.

(iv) Loss Tangent tan δ_2. Except for the lowest frequencies, where the data scatter is too large, the loss tangent tan δ_2 shows a similar continuous increase with increasing temperature and decreasing frequency as tan δ_1. Superimposed on this feature is a relaxation peak with the typical frequency-temperature shift which correlated with the step in ε_{33}^{T} and with the lower of the two relaxation peaks in tan δ_1.

In Table 1 the room temperature values of the dielectric constants ε_{11}^{T} and ε_{33}^{T} are listed as a function of frequency. It

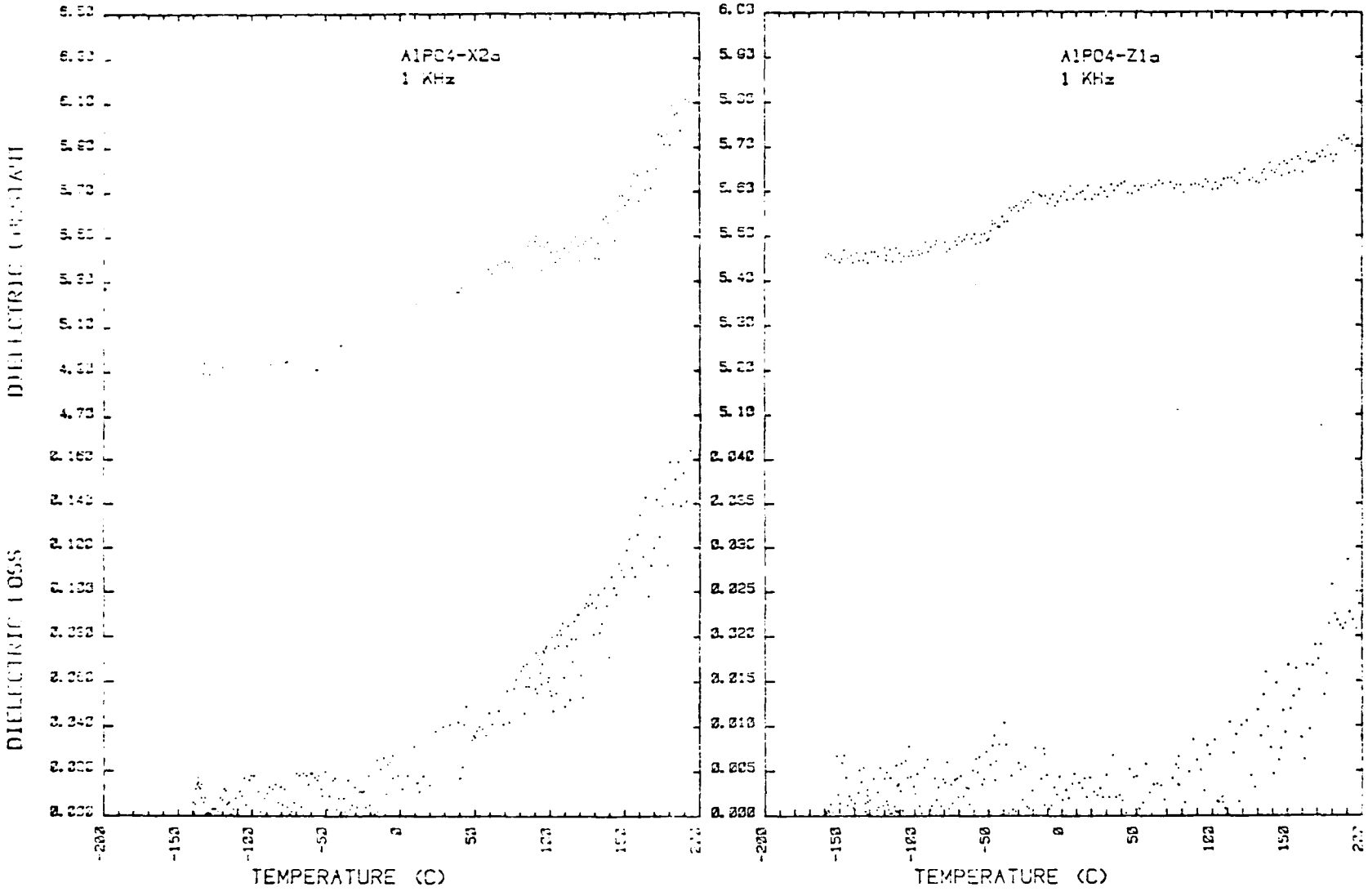

Figure 6. Relative Dielectric Constant ε^T and Loss Tangent of α-Berlinite versus Temperature at 1 kHz
(a) X-cut (b) Z-cut

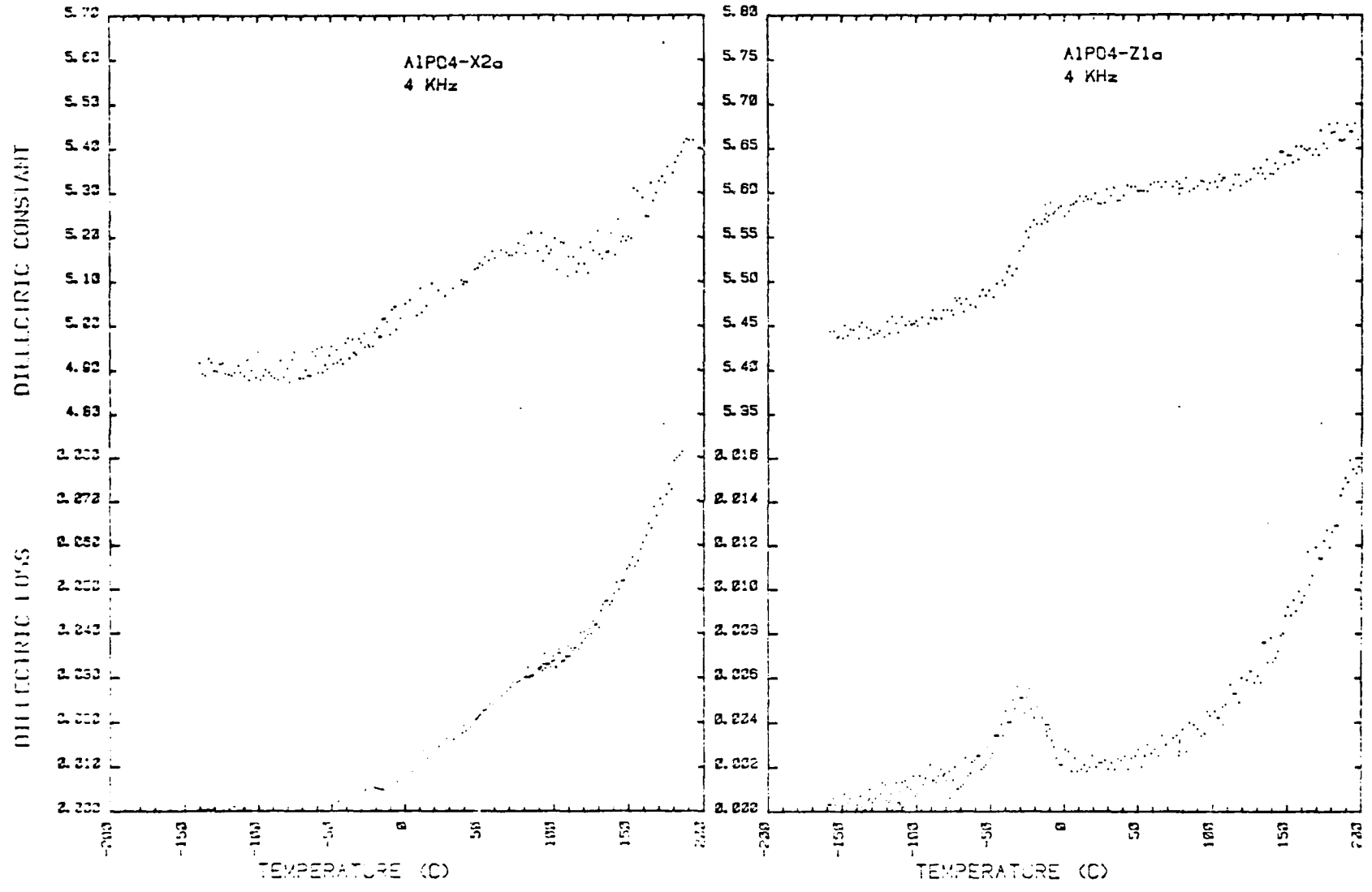

Figure 7. Relative Dielectric Constant ε^T and Loss Tangent of α-Berlinite versus Temperature at 4 kHz
(a) X-cut (b) Z-cut

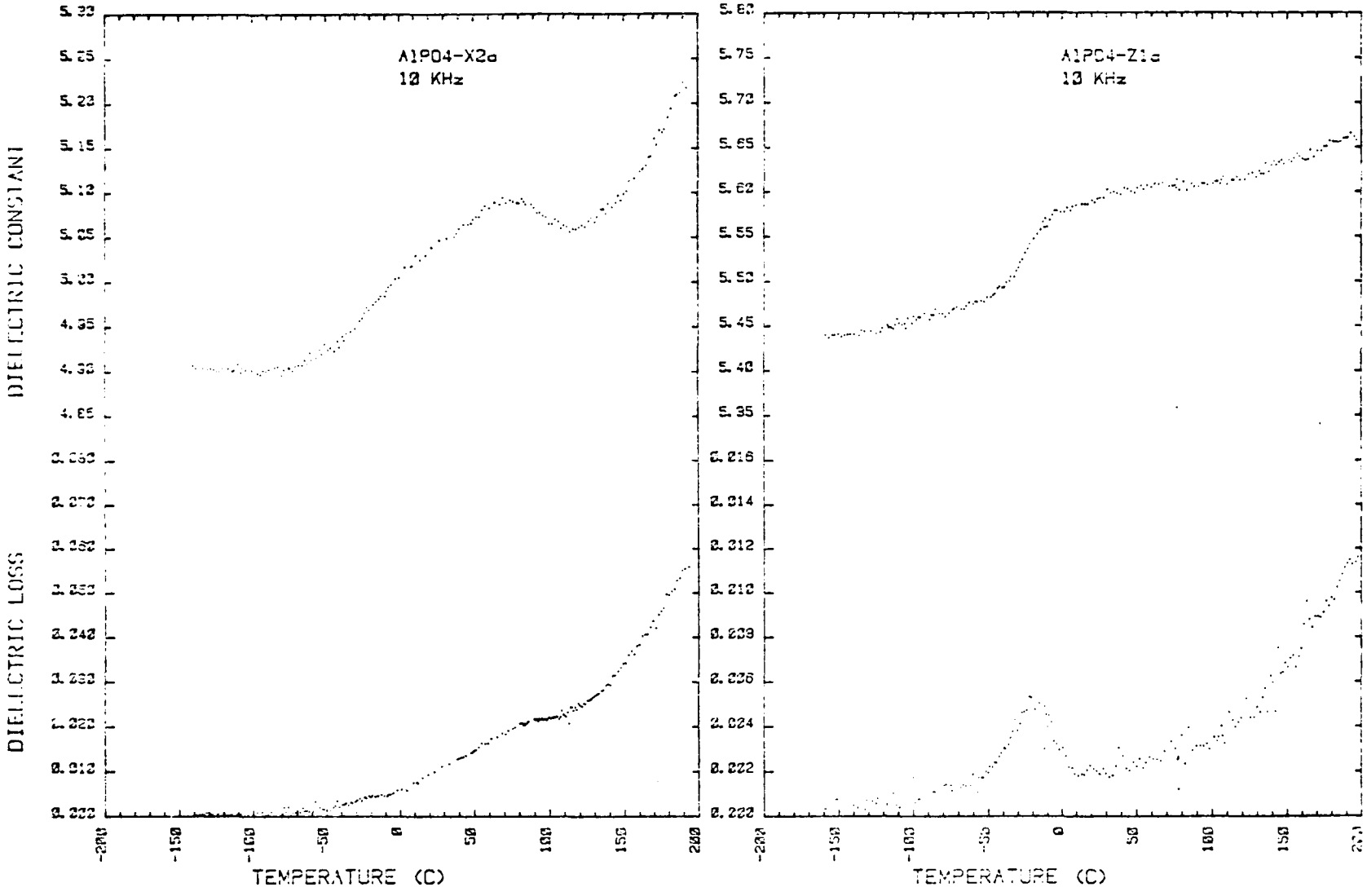

Figure 8. Relative Dielectric Constant ϵ^T and Loss Tangent of α-Berlinite versus Temperature at 10 kHz
(a) X-cut (b) Z-cut

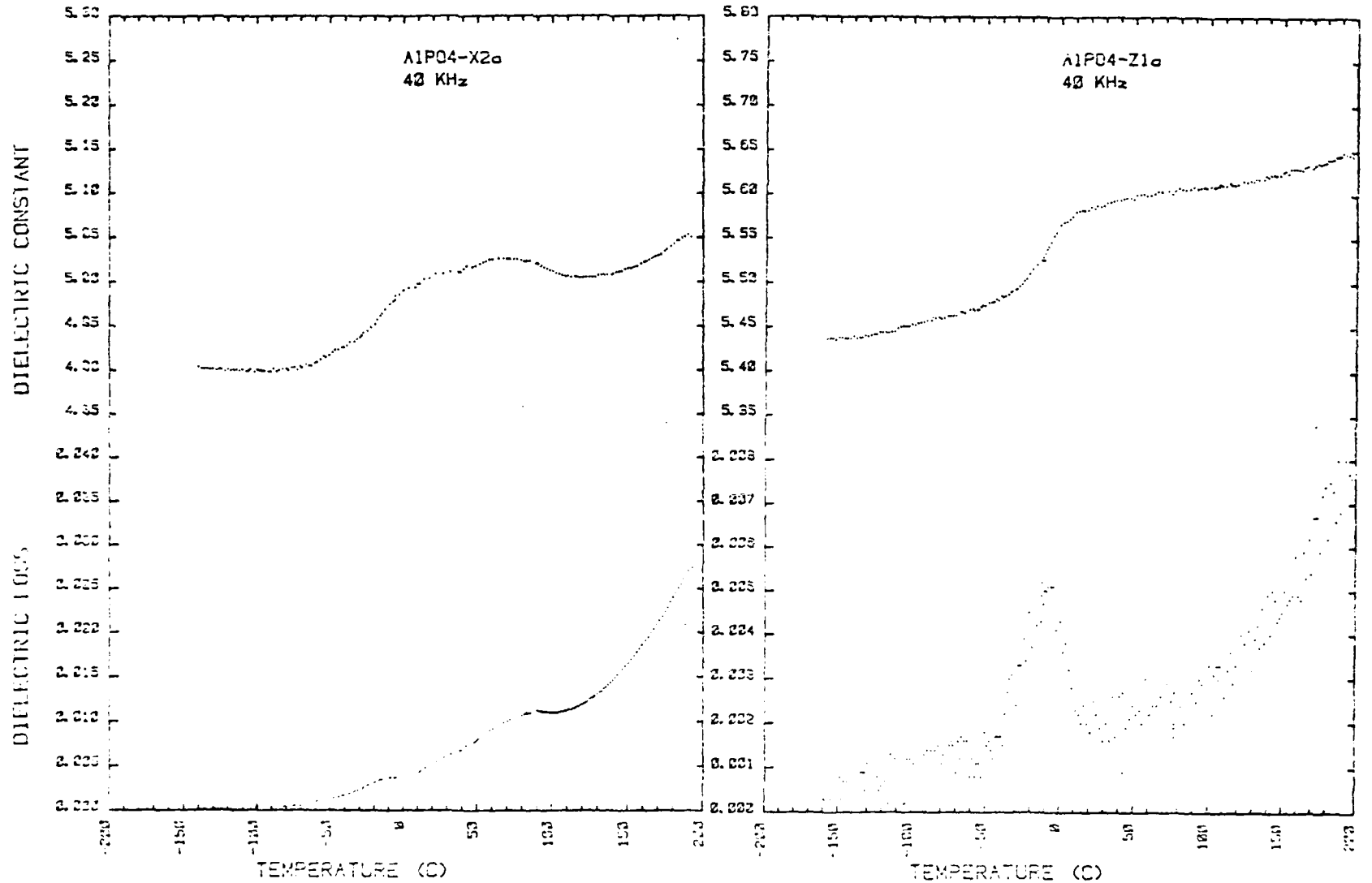

Figure 9. Relative Dielectric Constant ε^T and Loss Tangent of α-Berlinite versus Temperature at 40 kHz
(a) X-cut (b) Z-cut

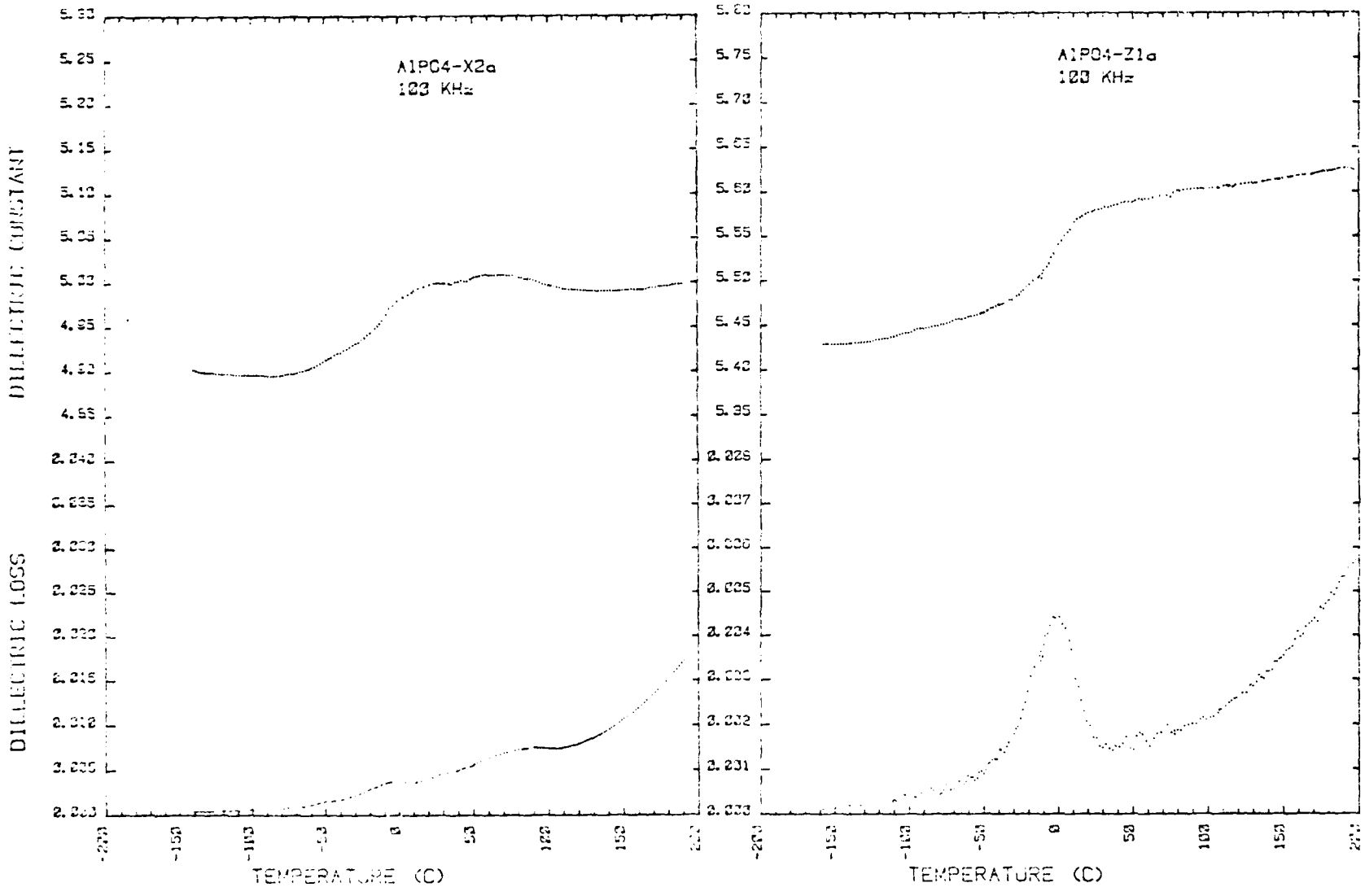

Figure 10. Relative Dielectric Constant ε^T and Loss Tangent of α-Berlinite versus Temperature at 100 kHz
(a) X-cut (b) Z-cut

Table 1. Free relative dielectric constants ε_{11}^{T} and ε_{33}^{T} of α-berlinite at 25°C for ten frequencies

Frequency	ε_{11}^{T}	ε_{33}^{T}
10^2	5.5	5.6
1.2×10^2	5.5	5.5
2×10^2	5.5	5.6
4×10^2	---	5.6
10^3	5.2	5.6
2×10^3	5.14	5.6
4×10^3	5.09	5.59
10^4	5.05	5.59
2×10^4	5.03	5.59
4×10^4	5.01	5.60
10^5	5.00	5.58

is apparent that in the frequency range from 10^2 to 10^5 Hz ε_{11}^T decreases by about 10 percent, and that ε_{33}^T remains virtually constant.

A Cole-Cole plot of the real imaginary parts of ε_{33}^T gives for the relaxation time

$$\tau = \tau_o e^{-Q/kt} \qquad (1)$$

with $\tau_o = 1.3 \times 10^{-18}$ sec, $Q = 1.05$ eV.

Comparison of the above results with those reported before (Barsch and Spear 1979) shows that the temperature dependence of ε_{33}^T is very similar, but that the absolute magnitude of the new value is smaller than those reported before.

The most puzzling feature in the present measurement is the occurrence of the two shallow minima of ε_{11}^T and the one shallow minima of ε_{33}^T. These minima cannot be explained by the stardard theory of dielectric properties. There is some evidence that the low temperature minimum, which is apparent in both ε_{11}^T and ε_{33}^T, could arise from condensation of water (or ice) on the platelet specimen. In fact, if data are taken with increasing temperature on samples previously exposed to air the dielectric constant measured initially is too large and decreases to a limiting value as the temperature is kept constant, but no such behavior is observed with decreasing temperature. This behavior could perhaps be attributed to the surface desorption of water from the specimen. On the other hand, the high temperature minimum of ε_{11}^T, which is not present in ε_{33}^T, and which is observed with the temperature decreasing, could be related to adsorption of water and concurrent diffusion into the open channels of the berlinite

structure. These channels run parallel to the c-axis and are exposed to air in the X-cut specimen, but not in the Z-cut specimen. Further measurements of the dielectric properties at elevated temperature in an inert-gas atmosphere are required to settle this question.

3.1.2 Electrical Conductivity

In order to identify the microscopic origin of the dielectric relaxation phenomena observed both in Z-cut and X-cut platelets of α-$AlPO_4$ the electrical resistivity of the specimens used before for the dielectric measurements was measured with a Keithley Model 616 Digital Electrometer.

For the Z-cut platelet (grown hydrothermally at the Naval Weapons Center, China Lake, California) a room temperature value of $\rho = 1.6 \times 10^{10}$ Ohm m was obtained from measurements at zero current, and an activation energy of $Q = 0.88$ eV was determined from measurements at constant voltage vs. temperature. Measurements on the X-cut sample (grown hydrothermally at the U.S. Signal Corps Engineering Labs., Fort Monmouth, New Jersey) gave similar results.

Calculating the loss tangent from the standard formula

$$\tan \delta = \frac{1}{\rho \omega \varepsilon_1} \qquad (2)$$

(ε_1 = real part of dielectric constant, ω = angular frequency) gives with the value of ρ according to (1) for a frequency of 1 MHz a value of $\tan \delta = 1.8 \times 10^{-9}$. This value is considerably smaller than the high temperature background measured at 300K and 1 MHz, which is of the order of 5×10^{-4} (Barsch and Spear, 1979; Fig. 10d). Hence one may conclude that the rise of the

dielectric loss at high temperature is not caused by the bulk conductivity of the crystal. This conclusion is substantiated by the relatively weak temperaure variation of the high temperature rise of tan δ which would correspond to an activation energy much smaller than that given above. Thus it appears that the high temperature rise of the dielectric loss may be attributed, as the relaxation peak(s) observed at lower temperature, to defect relaxation or to the effect of conducting inclusions. This conjecture should be subjected to further investigation by means of dielectric loss measurements versus temperature at frequencies below 1 kHz, which should reveal a maximum of tan δ below 250°C.

In order to test the hypothesis that the dielectric relaxation phenomena observed arise from conducting inclusions one may use the formulae for the real and imaginary parts of the dielectric constant, ε' and ε'', of a non-dissipative dielectric medium characterized by a relative dielectric constant ε_1' and ε_1'' = 0, with spherical inclusions of a medium with the electrical conductivity σ (Daniel, 1967):

$$\varepsilon' = \varepsilon_\infty + \frac{\varepsilon_1' N}{1 + (\omega\tau)^2} \tag{3a}$$

$$\varepsilon'' = \frac{\varepsilon_1' \omega\tau}{1 + (\omega\tau)^2} \tag{3b}$$

where

$$\tau = \frac{2\varepsilon_1' \varepsilon_0}{\sigma} \tag{4}$$

(ε_0 = vacuum dielectric constant) and

$$N = 4.5q. \quad (5)$$

q denotes the volume fraction of the spherical inclusion.

By applying these equations to the relaxation peak which is present in both the X-cut and Z-cut crystals one obtains for the volume fraction of inclusions the value $q = 2.3 \times 10^{-3}$ and for the resistivity of the inclusions $\rho = 3.0 \times 10^{3}$ Ohm m. Both values are plausible for growth related inclusions. For the high temperature contribution to the loss tangent one obtains for the Z-cut specimen for a volume fraction of inclusions similar to the above value resistivity values of the same order of magnitude. Further studies on crystal growth and characterization would be required in order to identify the nature of the inclusions and, if necessary, to eliminate them in the crystal growth process.

3.1.3 Piezoelectric Constants

An ultrasonic AC capacitance dilatometer has recently been developed in this laboratory by Professor L. E. Cross and collaborators (Uchino and Cross, 1979) and is used to measure the piezoelectric strain constant d_{11} on two X-cut samples of α-berlinite under ONR Contract No. N00014-78-C-0291. In Table 2 the results are compared with the earlier results obtained from the analysis of the ultrasonic data (Chang and Barsch, 1976) and from direct measurement by means of the x-ray method (Barsch and Spear, 1979). It is apparent that within the joint experimental error and the two values obtained with the AC dilatometer agree with each other and with the ultrasonically determined value. The actual values obtained with the dilatometer are, however, about 20 percent smaller than the ultrasonic value. On the other

Table 2. Comparison of piezoelectric strain constant d_{11} as measured by different techniques

Technique	Reference	d_{11} ($10^{-12}mV^{-1}$)
Ultrasonic	Chang and Barsch, 1976	5.3 ± 1.6
X-ray	Barsch and Spear, 1979	11.7 ± 0.4
AC Dilatometer	Uchino and Cross, 1979	3.98 ± 0.05[a] 4.2 ± 0.2[b]

[a]Sample previously used for ultrasonic measurements (Chang and Barsch, 1976).

[b]Sample previously used for x-ray determination of piezoelectric constants (Barsch and Spear, 1979).

hand, the x-ray value is over two times larger than the ultrasonic value and almost three times as large as the dilatometer value. Thus one may tentatively conclude that the x-ray value is subject to a large systematic error of unknown origin. Perhaps electric field enhancement effects near inclusions or voids, or space charge effects near the electroded surface may be responsible for this.

If the smaller dilatometer value of d_{11} is accepted as correct one may expect that for α-berlinite the maximum electromechanical coupling factor k for bulk waves is roughly 20 percent smaller than previously indicated (Chang and Barsch, 1976), although still larger than for α-quartz. This is corroborated by the direct measurement of the coupling factor k^2 for surface waves, for which a value of only half of the

theoretically predicted value, but almost twice as large as for ST quartz was found (O'Connell and Carr, 1978).

In order to predict the maximum coupling factor for the temperature compensated directions more accurately, more reliable values of the piezoelectric strain constant d_{14} and more data on the effect of crystal imperfections on the piezoelectric and dielectric constants and the temperature derivatives of these quantities are required.

3.2 Bismuth Titanate and Lead Bismuth Niobate

Bismuth titanate, $Bi_4Ti_3O_{12}$ (BT), and lead bismuth niobate, $PbBi_2Nb_2O_9$ (PBN) are both members of a family of bismuth oxide layer compounds of composition $(Bi_2O_2)^{+2}(Me_{m-1}R_mO_{3m+1})^{-2}$, where Me denotes a mono-, di- or trivalent cation, R = Ga^{+3}, Ti^{+4}, Nb^{+5} or Ta^{+5}, m = 2, 3, 4, 5, in which m perovskite-like layers of nominal composition $MeRO_3$ are stacked between Bi_2O_2 layers along a pseudo-tetragonal c-axis. These compounds were first synthesized and their structure was determined by Aurivillius (1949 a,b). Ferroelectricity in this group of compounds was discovered by Smolenski, et al. (1959). For $PbBi_2Nb_2O_9$ it is Me = Pb, R = Nb and m = 2, and ferroelectric Curie temperatures from 526° to 560°C have been reported for ceramic specimens (Smolenski, et al., 1959; Subbaro, 1962). For $Bi_4Ti_3O_{12}$ it is Me = Bi, R = Ti, and m = 3, and the Curie temperature lies between 643° and 675°C (Van Uitert and Egerton, 1961; Subbaro, 1961). Because of the identical electron configurtions of Bi^{+3} and Pb^{+2} property differences between the two compounds should result only from different number of peroskite-like layers (m = 2 and 3,

respectively). On the whole, one may expect the properties of PBN to correspond more closely to those of Bi_2O_3, and those of BT to be more perovskite-like. Because of the common layer structure one may expect the properties of PBN and BT to be qualitatively similar.

With the exception of BT virtually all property measurements on this class of compounds were obtained from ceramic polycrystal specimens, and mostly X-ray studies and dielectric constant measurements are available (Aurivillius, 1949 a, b; Ismailzade, 1960; Smolenski, et al., 1959; Subbarao, 1962). No elastic or thermoelastic constant data were available for any of these layer compounds.

The occurrence of ferroelectricity for the members of this family of compounds is mostly inferred from the Curie-Weiss behaviour of the polycrystal dielectric constant, but for a few ceramic specimen and for single crystal BT dielectric hysteresis has also been observed (Subbarao, 1961; Subbarao, 1962; Van Uitert and Egerton, 1961). For PBN (ceramic) no hysteresis behaviour for electric fields up to 50 kV/cm and for temperatures from 100 to 250° has been found (Smolenski, et al., 1959; Subbarao, 1962), but ceramic PBN could be poled by fields from 20 to 50 kV/cm and temperatures ranging from 200 to 250°C (Subbarao, 1962). For the poled ceramic PBN a piezoelectric constant of $d_{33} = 1.5 \times 10^{-11}$ C/N has been measured (Subbarao, 1962). For PBN and other members of this family of compounds the peak in the dielectric constant (the maximum observed for PBN was $\epsilon_{max} = 2{,}100$) coincides with a structural phase transformation from

tetragonal to orthorhombic symmetry (Ismailzade, 1960). Except for BT the direction of the spontaneous polarization $\bar{P}_s$ is not known. For BT $\bar{P}_s$ lies approximately in the perovskite layer, deviating by an angle of 5° from the a-axis, and has the components P_a = 50 $\mu C/cm^2$ and P_c = 4 $\mu C/cm^2$ (Cummins and Cross, 1968). For BT a hysteresis in the c-direction has been observed at room temperature with a coercive field of about 6 kV/cm, but no hysteresis was found in the plane perpendicular to c (Van Uitert and Egerton, 1961). However, BT can be poled in the a-direction by an elaborate high temperature poling technique (Hopkins and Miller, 1970).

3.2.1 Elastic Constants of Bismuth Titanate

The high temperature paraelectric phase of BT belongs to the tetragonal space group I4/mmm (C^9_{4v}). At room temperature x-ray and neutron diffraction data are consistent with a polar orthorhombic structure of space group B2cb (C^{17}_{2v}) with lattice parameters of a = 5.448Å and c = 32.83Å (Dorrian, et al., 1971). There are four formula units per unit cell. The structure consists of $Bi_2O_2^{+1}$ layers which alternate with perovskite-like $Bi_2Ti_3O_{10}$ layers (Aurivillius, 1950). From measurements of the optical indicatrix as a function of temperature the actual crystal symmetry may be established to be monoclinic (Cummins and Cross, 1968), but the structural deviations from orthorhombic symmetry are so small that they do not show up in X-ray or neutron diffraction masurements (Dorrian, et al., 1971).

There are over 50 ferroelectric compounds known which belong to the bismuth titanate family (Newnham, et al., 1971). Only dielectric and optical data, but no elastic and piezoelectric

constant data are available so far. In order to examine the suitability of $Bi_4Ti_3O_{12}$ as a substrate for temperature compensated SAW devices we have begun measurements of the elastic constants of this material as a function of temperature. A single crystal platelet of linear dimensions of about 5x4x0.75 mm^3 was used for this purpose. The crystal had been grown by S. E. Cummins, Wright-Patterson Air Force Base, Ohio, by means of a flux method (Pulvari, 1964) and was of brown color and optically translucent. No attempts to pole the crystal have been made. The transit time of a shear wave propagating in the c-direction (the platelet normal), polarized in a direction 45° from the a-or b-axis, has been measured by means of the ultrasonic pulse echo method from 10K to 315K. Because of the near-tetragonality of the crystal structure the results for polarization in the a- or b-direction are expected to be very similar. In Figure 11 the transit time for this mode is plotted versus temperature. It exhibits the usual positive slope, implying a negative temperature coefficient of the average elastic shear modulus $(c_{44} + c_{55})/2$. In order to establish the suitability of BT for temperature compensated SAW devices the remaining elastic constants must be determined as a function of temperature. Since the available single crystals are all in the form of thin platelets the resonance technique has to be used for this purpose. Because of the time-consuming sample preparation this work was not pursued under the present contract.

3.2.2 Elastic and Dielectric Constants of Lead Bismuth Niobate

As a result of the crystal growth efforts under the present contract, PBN is the only member of the entire family of bismuth

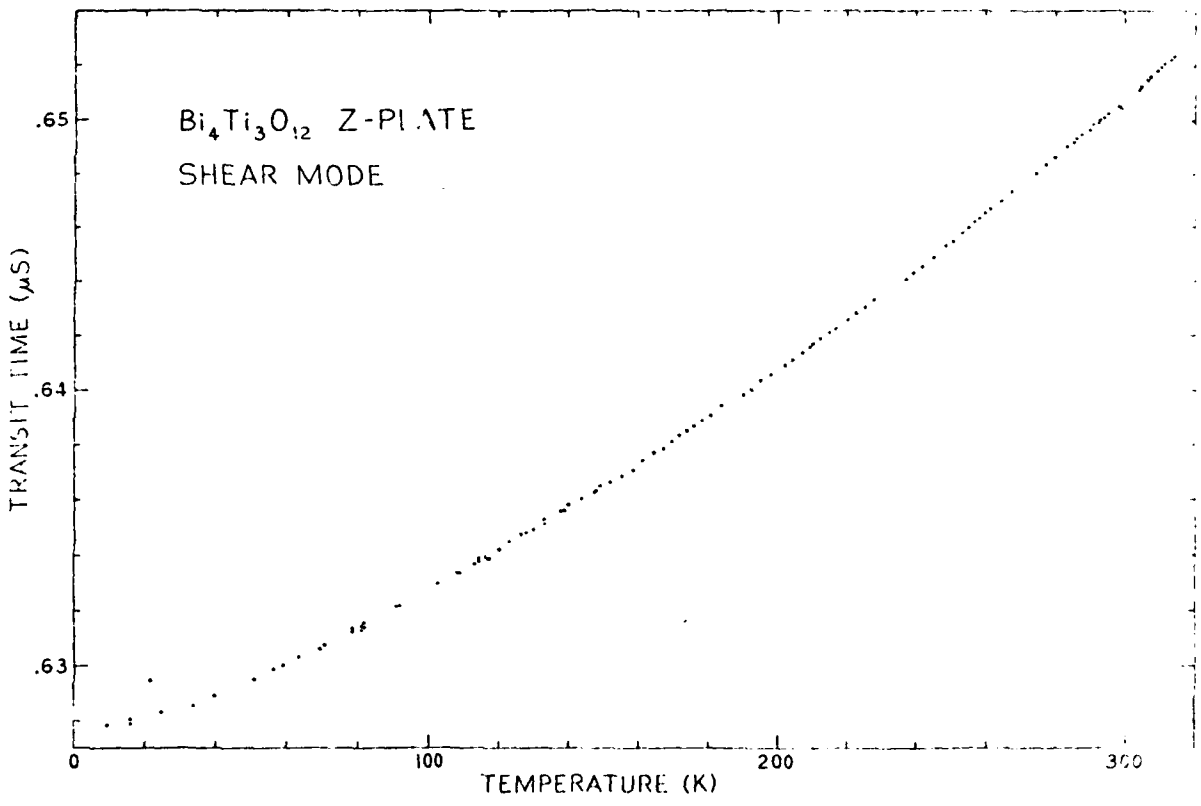

Figure 11. Transit time of shear mode propagating in c-direction for $Bi_4Ti_3O_{12}$ versus temperature.

layer compounds for which single crystal boules with centimeter dimensions along all three crystallographic axes have become available. However, PBN exhibits easy cleavage of the (001) planes and the cutting, orienting and polishing of the crystals turned out to be extraordinarily difficult and time consuming if cleavage was to be avoided. Especially detrimental was the propensity of thin c-cut platelets to flake near edges and corners of their flat a-cut surfaces, thereby nullifying the cumbersome sample preparation effort, often in its final stage. Whereas c-cut platelets could be cut and polished more easily it was only after several months of effort that (as yet unpolished) a-cut platelets have been obtained. This was achieved by surrounding the oriented and glass-mounted sample in DUCO cement prior to cutting and using cutting rates of less than one millimeter per day with a vibration free wiresaw (diameter of string 0.010 inch). We have started to use HYSOL-cement, previously successfully used by Cummins and Cross (1968) and expect that, because of its greater rigidity it will provide still better protection of the sample than DUCO-cement. At the time of the expiration of the present contract (6/30/80) the (100) faces of the a-cut samples had not yet been polished. Dielectric constant measurements were possible with these unpolished samples, but ultrasonic velocity measurements with the pulse superposition method could not be made for lack of good echos.

A c-cut platelet of unpoled PBN of thickness 2.591 mm was prepared for the elastic constant measurements. The transit time of the longitudinal and of the two transverse acoustic waves

propagating in the c-direction were measured as a funtion of temperature from about 0°C to about 50° to 90°C by means of the ultrasonic pulse superposition method. In Figures 12, 13a and 13b the elastic constants c_{33}, c_{55} and c_{66} obtained from these data are plotted versus temperature. All three moduli are seen to have the usual negative slope. The data for the two shear moduli are virtually identical. Although these results will be somewhat different for poled specimens, no drastic changes, especially no positive temperature coefficient for any of these three moduli is to be expected. Of course, for assessing the existence of temperature compensated directions the remaining six elastic constants and the set of piezoelectric constants must be known versus temperature.

Dielectric measurements were made on a (polished) c-cut platelet of thickness 0.391 mm and on an (unpolished) a-cut platelet of thickness 0.4818 mm. For the c-cut sample no hysteresis was found at room temperature with a Sawyer and Tower circuit in electric fields up to 25 kV/cm. Also no response with a d_{33}-meter was obtained, indicating that the piezoelectric constant $d_{33} < 10^{-12}$C/N. The results may be interpreted so as to indicate that PBN, unlike BT, has no component of the spontaneous polarization along the c-axis, or, alternatively, but less likely, that at R.T. the coercive field $E_c > 25$ kV/cm. Further dielectric studies at higher fields and/or elevated temperature are required to settle this question. For the a-cut platelet a weak hysteresis loop was observed at room temperature in an

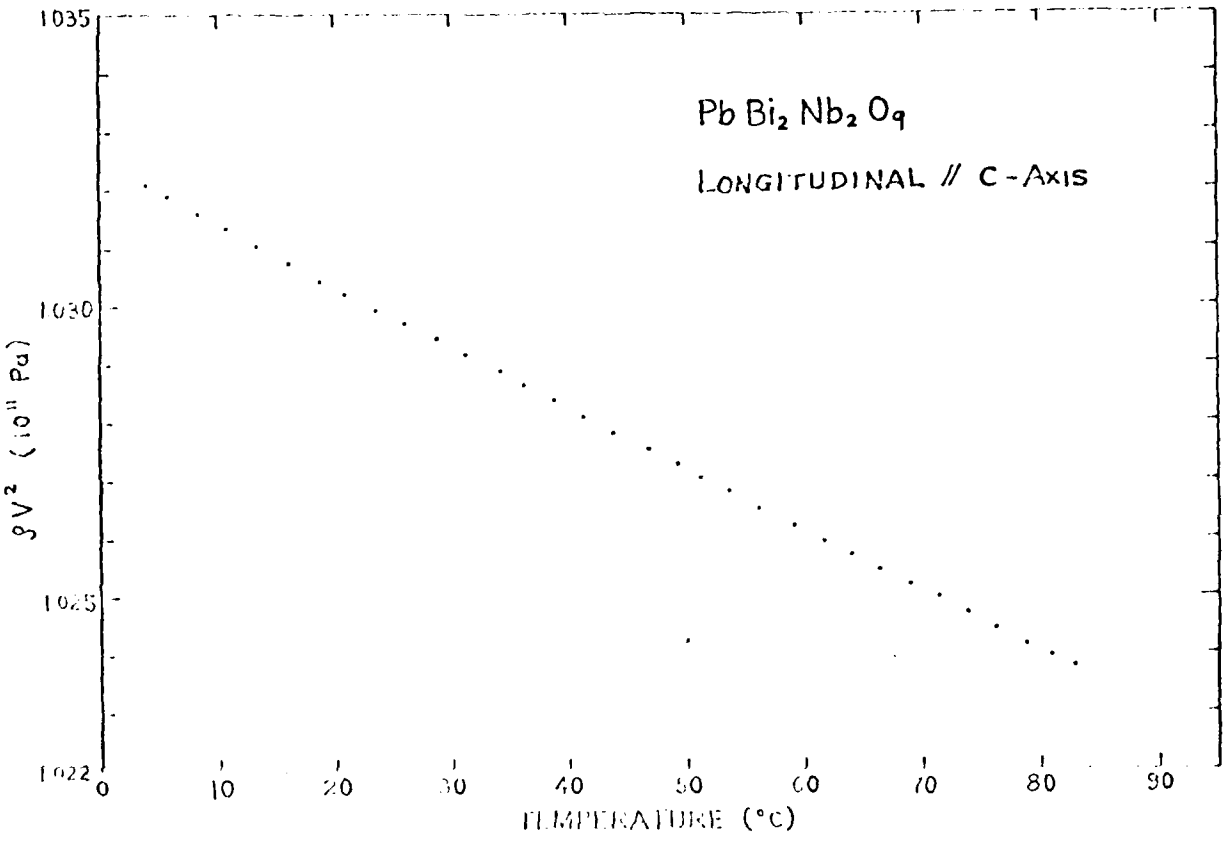

Figure 12. Longitudinal elastic constant c_{33} of unpoled PBN versus temperature.

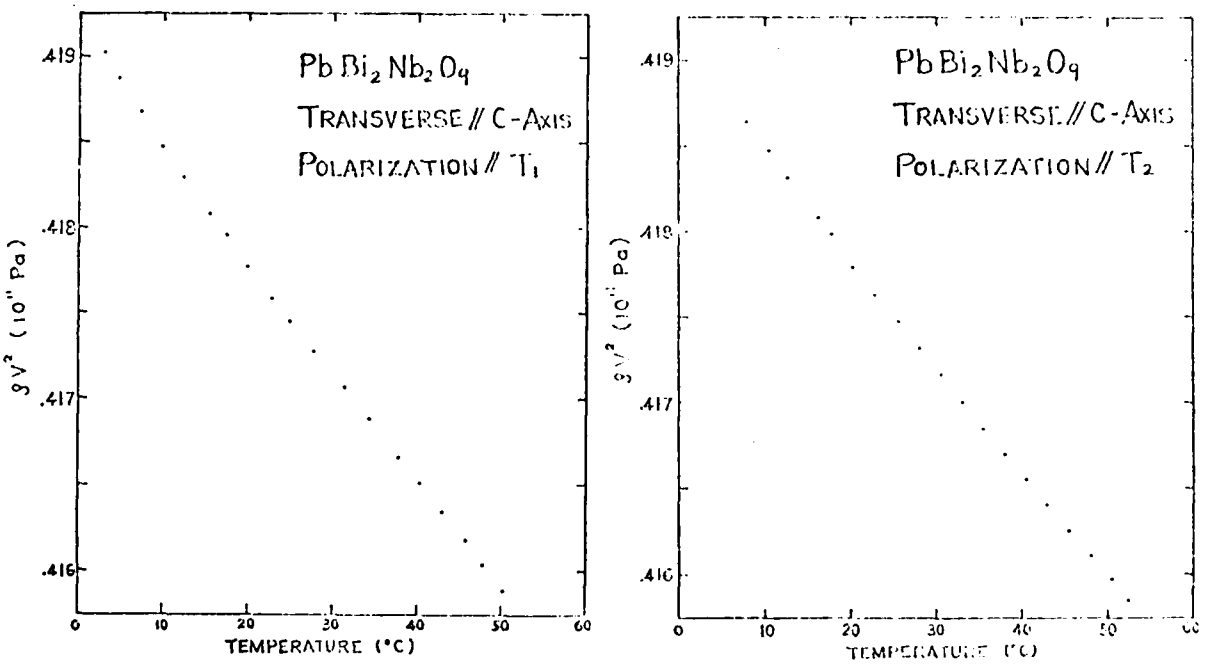

Figure 13. Shear constants c_{55} (a) and c_{66} (b) of unpoled PBN versus temperature.

electric field of 16.6 kV/cm. As shown in Figure 14 at elevated temperatures the loop widens. While the shape of the loop and its temperature dependence seem to suggest the presence of a conductivity loss mechanism contributions from a ferroelectric hysteresis cannot be ruled out.

The dielectric constant and the loss tangent have been measured for the (unpoled) a-cut sample at 10^3, 10^4, 10^5 and 10^6 Hz from room temperature to 200°C. The results for 1 kHz and 1 MHz are shown in Figure 15a and 15b and indicate that in the temperature range to 200°C the dielectric constant ε_a^T almost doubles from the room temperature value of 210 to 260. The loss tangent rises more slowly. The absolute magnitude of ε_a^T at R.T. is consistent with the polycrystal results of Subbaro (1962) who obtained a value of ε = 170 at 25 K. However, the rise in temperature of ε_a^T is much more rapid than for the polycrystal sample, where the doubling of ε occurs over a temperature interval of 400 K. The relatively fast rise of ε_a^T is consistent with the occurrence of a maximum of ε = 2,100 in the polycrystal, which naturally has been attributed to the ferroelectric transition. Although Subbarao (1962) concludes that the spontaneous polarization is in the c-direction the above results on PBN and the structural similarity with BT suggest that the main component of P_s is perpendicular to this direction. More experimental effort would be required to fully characterize all pertinent properties of PBN.

(a)

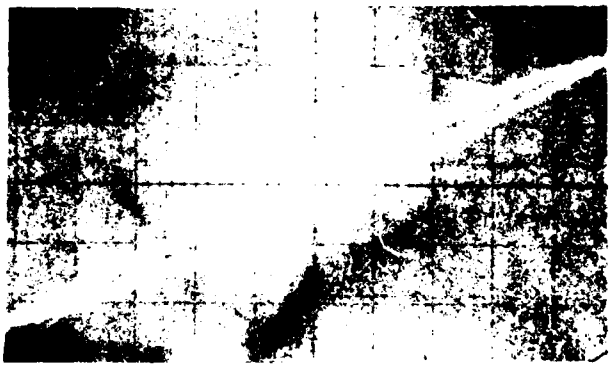

(b)

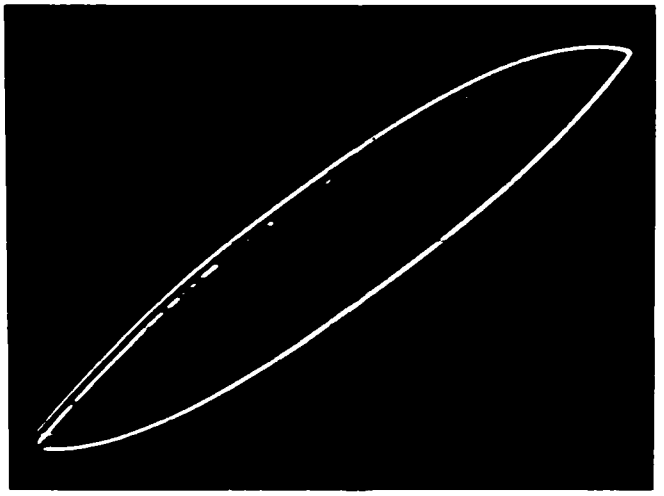

(c)

Figure 14. Dielectric hysteresis of a-cut PBN at 10Hz. (a) 24.5°C; (b) 86.6°C; (c) 192.5°C. Horizontal scale corresponds to 200 V/division, vertical scale to 50 V/division.

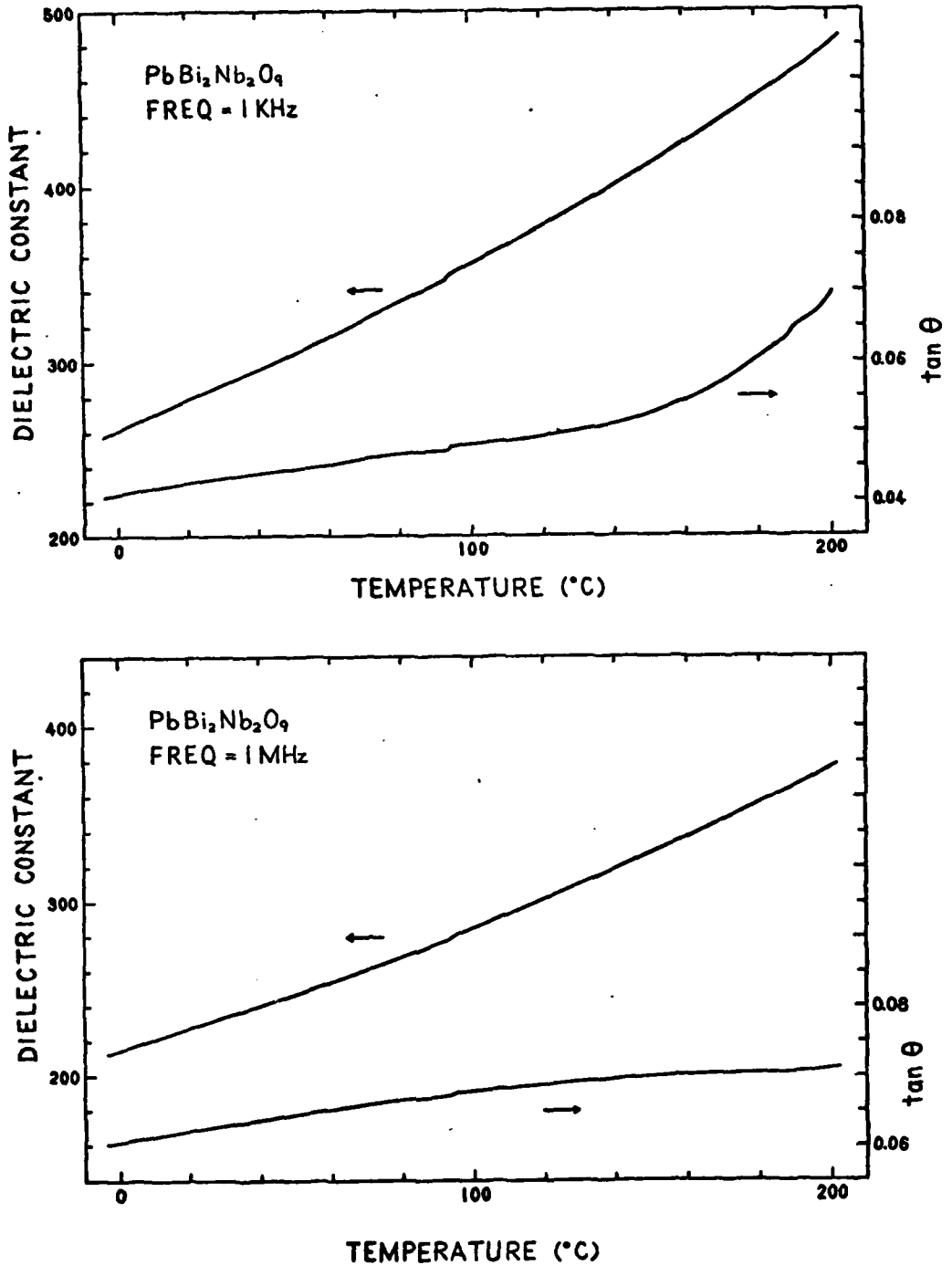

Figure 15. Relative Dielectric Constant ε_a^T and loss tangent for PBN versus temperature.
(a) 1 kHz (b) 1 MHz

4. Conclusions

The results obtained under the present contract indicate that temperature compensated performance and large electromechanical coupling factors in ultrasonic bulk and surface wave devices are not mutually exclusive, and that the performance characteristics of presently used acoustic wave devices are not yet optimized with respect to the choice of the best possible material. The results indicate further that the approach used in our systematic search for new temperature compensated piezoelectric materials with larger piezoelectric coupling than α-quartz has been very successful. This approach led to the identification of α-berlinite and lead potassium niobate as superior substitutes for α-quartz and consisted of the following four steps:

(1) Selection of promising candidate materials on the basis of heuristic criteria,

(2) Growth of single crystal specimen sufficiently large for physical property measurements,

(3) Measurement of the complete set of the elastic, piezoelectric, dielectric and thermoelastic constants,

(4) Computer calculations to determine the temperature compensated directions and their associated coupling factos for bulk and surface acoustic waves.

It is to be expected that through a continued systematic search new materials with still better properties could be found.

5. Recommendations

Since α-berlinite and lead potassium niobate have been found to be superior to α-quartz for bulk and surface wave applications it would be appropriate to continue work on both materials in order to optimize their properties. This would involve a systematic study and better control of the crystal growth parameters required for production of high-quality crystals, and further investigations on the effect of crystal imperfections and chemical composition on the properties and performance.

In addition, it appears promising to continue the systematic search for new temperature compensated materials on the basis of the approach used previously, which could lead to the discovery of other materials with still better properties. Specifically, it is recommended to continue crystal growth efforts for subsequent properties measurements on Li_2SiO_3, Bi_2MoO_6, and Bi_2MoO_6-Bi_2WO_6 solutions in addition to lead potassium niobate.

6. References

B. Aurivillius (1949a). Mixed Bismuth Oxides with Layer Lattices: I, Structure Type of $CaCb_2Bi_2O_9$, Arkiv Kemi, 1 [54], 463-80 (in English).

B. Aurivillius (1949b). Mixed Bismuth Oxides with Layer Lattices: II, Structure of $Bi_4Ti_3O_{12}$, Arkiv Kemi, 1 [58], 499-512 (in English).

G. R. Barsch and R. E. Newnham (1975). Piezoelectric Materials with Positive Elastic Constant Temperature Coefficients, Final Report AFCRL-TR-75-0163, Contract No. F19628-73-0108.

G. R. Barsch and K. E. Spear (1977). Temperature Compensated Piezoelectric Materials, RADC-TR-77-179; Final Technical Report on Contract No. F19628-75-C-0085, A044237.

G. R. Barsch and K. E. Spear (1979). Temperature Compensated Piezoelectric Materials, RADC-TR-79-219; Final Technical Report on Contract No. F19628-77-C-0131, A077650.

Z. P. Chang and G. R. Barsch (1976). Elastic Constants and Thermal Expansion of Berlinite, IEEE Proc. Sonics Ultrasonics SU23, 127-135.

S. E. Cummins and L. E. Cross (1968). Electrical and Optical Properties of Ferroelectric $Bi_4Ti_3O_{12}$ Single Crystals, J. Appl. Phys. 39, 2268-2274.

V. V. Daniel (1967). Dielectric Relaxation, Chapter 14, Academic Press, London and New York.

J. F. Dorrian, R. E. Newnham, D. K. Smith and M. I. Kay (1971). Crystal Structure of $Bi_4Ti_3O_{12}$, Ferroelectrics 3, 17-27.

M. M. Hopkins and A. Miller (1970). Preparation of Poled, Twin-Free Crystals of Ferroelectric Bismuth Titanate, $Bi_4Ti_3O_{12}$, Ferroelectrics 1, 37-42.

I. G. Ismailzade (1960). X-Ray Study of Structure of Some New Ferroelectrics with Layer Structure. Izvest. Acad. Nauk SSSR, Ser Fiz. 24 [10], 1138-1202, Engl. Transl: Bull. Acad. Sci. USSR, Phys. Ser. 2, 1201-1206.

R. E. Newnham, R. W. Wolfe and J. F. Dorrian (1971). Structural Basis of Ferroelectricity in the Bismuth Titanate Family, Mat. Res. Bull. 6, 1029-1040.

R. M. O'Connell and P. H. Carr (1978). New Materials for Surface Acoustic Wave Devices, 1978 Ultrasonics Symposium Proceedings, IEEE Cat. #78 CH 1344-1SU.

C. F. Pulvari (1964). Air Force Avionics Laboratory, Tech. Rept. 62-124 (May 1964), Wright Patterson Air Force Base, Ohio.

G. A. Smolenski, V. A. Isupov and A. I. Agranovskaya (1959). Fizika Tverdogo Tela 1, 169-170. Engl. Transl.: Soviet Physics - Solid State 1, 149-150.

E. C. Subbarao (1961). Ferroelectricity in $Bi_4Ti_3O_{12}$ and its Solid Solutions, Phys. Rev. 122, 804-807.

E. C. Subbarao (1962). A Family of Ferroelectric Bismuth Compounds, J. Phys. Chem. Solids 23, 665-676.

K. Uchino and L. E. Cross (1979). A High-sensitivity AC Dilatometer for the Direct Measurement of Piezoelectricity and Electrostriction, 33rd Annual Symposium on Frequency Control, Atlantic City, New Jersey.

L. G. Van Uitert and L. Egerton (1961). Bismuth Titanate. A Ferroelectric, J. Appl. Phys. 3, 959.

MISSION
of
Rome Air Development Center

RADC plans and executes research, development, test and selected acquisition programs in support of Command, Control Communications and Intelligence (C^3I) activities. Technical and engineering support within areas of technical competence is provided to ESD Program Offices (POs) and other ESD elements. The principal technical mission areas are communications, electromagnetic guidance and control, surveillance of ground and aerospace objects, intelligence data collection and handling, information system technology, ionospheric propagation, solid state sciences, microwave physics and electronic reliability, maintainability and compatibility.

Printed by
United States Air Force
Hanscom AFB, Mass. 01731


ATF